Mechanical behaviour'sevolution of a PLA-b-PEG-b-PLA triblock copolymer during hydrolytic degradation

Quentin Breche, Grégory Chagnon, Guilherme Machado, Edouard Girard, Benjamin Nottelet, Xavier Garric, Denis Favier

Mechanical behaviour's evolution of a PLA-b-PEG-b-PLA triblock copolymer during hydrolytic degradation

Q. Breche[a,b], G. Chagnon[a,b,*], G. Machado[a,b], E. Girard[a,b], B. Nottelet[c], X. Garric[c], D. Favier[a,b]

[a]Université Grenoble-Alpes, TIMC-IMAG, F-38000 Grenoble, France

[b]CNRS, TIMC-IMAG, F-38000 Grenoble, France

[c]Université de Montpellier, Faculté de pharmacie/Institut des biomolécules Max Mousseron (IBMM)/CNRS/UMR5247, 34093 Montpellier, France

PLA-b-PEG-b-PLA is a biodegradable triblock copolymer that presents both the mechanical properties of PLA and the hydrophilicity of PEG. In this paper, physical and mechanical properties of PLA-b-PEG-b-PLA are studied during in vitro degradation. The degradation process leads to a mass loss, a decrease of number average molecular weight and an increase of dispersity index. Mechanical experiments are made in a specific experimental set-up designed to create an environment close to in vivo conditions. The viscoelastic behaviour of the material is studied during the degradation. Finally, the mechanical behaviour is modelled with a linear viscoelastic model. A degradation variable is defined and included in the model to describe the hydrolytic degradation. This variable is linked to physical parameters of the macromolecular polymer network. The model allows us to describe weak deformations but become less accurate for larger deformations. The abilities and limits of the model are discussed.

1. Introduction

Biodegradable polymers derived from lactid (LA), glycolide (GA) and ϵ-caprolactone are widely used in many biomedical applications such as implantable devices (Maurus and Kaeding, 2004), drug delivery systems (Ikada and Tsuji, 2000) and tissue engineering (Webb et al., 2004). The main advantage of biodegradable polymers is that they can be bioresorbable. It means that products of degradation are oligomers that can be metabolites which enter biochemical pathways or are excreted by the kidneys. Thus it avoids dramatic toxicity and long term problems due to the presence of synthetic materials in the organism (Chen et al., 2013). Among biodegradable biomaterials, due to its good mechanical properties, poly-lactic acid (PLA) is the most used for load bearing applications (Nair and Laurencin, 2007). Moreover, its crystalline rate and molecular weight can be easily

*Corresponding author at: Laboratoire TIMC-IMAG, Domaine de la Merci, 38706 La Tronche Cedex, France. Tel.: +33 0 4 56 52 00 86.
E-mail address: gregory.chagnon@imag.fr (G. Chagnon).

varied in order to modulate its mechanical properties (Perego et al., 1998). However, because of its hydrophobicity, the degradation rate of PLA is very low and its total resorption in vivo can take many years (Nair and Laurencin, 2007). Poly(ethylene glycol) (PEG), for its part, is well known for its hydrophilicity, water-solubility, lack of toxicity and excellent biocompatibility (Stefani et al., 2006). The interest of the association of PLA and PEG is that it combines the mechanical properties of PLA and the hydrophilicity of PEG. The association keeps the biodegradability and possess a better properties modulation. The variety of compositions offered by the PLA-*b*-PEG-*b*-PLA allows a very large range of mechanical properties and degradation times (Garric et al., 2012). That makes this polymer an excellent candidate for tissue engineering applications (Tessmar and Göpferich, 2007).

It exists two ways of degradation for biodegradable biomaterials in living organisms: enzymatic and hydrolytic. Enzymatic degradation appears, most of the time, on naturally occurring polymers like polysaccharides or proteins (Park et al., 2011). For aliphatic polyesters like PLA-*b*-PEG-*b*-PLA, the main degradation process is the hydrolysis of ester links. It starts when water diffuses into the polymer bulk leading to a swelling. The hydrolysis reaction cleaves the ester links in polymeric bonds leading to the creation of oligomers and monomers. Then, these monomers are released out of the polymer bulk causing characteristic mass loss and material erosion (Göpferich, 1996). The chain cleavage comes with the decrease of molar mass and generates an evolution of mechanical properties. When the polymeric structure thickness is important, an autocatalytic process can appear, accelerating local degradation. It generates carboxylic acids monomers, which stay locked in the polymeric matrix, lowering surrounding pH (Göpferich, 1996).

In order to design structures for different biomedical applications, especially in tissue engineering, a detailed knowledge of the material's mechanical behaviour and its evolution during degradation is essential (Chen et al., 2013). Different studies deal with mechanical properties like Young's modulus, tensile strength and elongation at break during hydrolytic degradation. These properties are very sensitive to crystallinity and initial structural parameters of the crystalline phase in the case of a semi-crystalline PLA (Tsuji et al., 2000; Tsuji and Ikada, 2000). However, many authors observed that it exists a period, especially for amorphous PLA, in the earlier stages of degradation, for which Young's modulus and tensile strength remain constant before decreasing (Tsuji, 2002; Karjalainen et al., 1996; Leroy et al., 2013). Li et al. (1990) measured the conservation modulus during in vitro degradation for semi-crystalline and amorphous PLA. They showed, as the same manner as the Young modulus, a latency period during which this one does not evolve in the amorphous case. This period does not exist when the polymer is semi-crystalline.

Few models dealing with the loss of mechanical properties during hydrolytic degradation can be found in the literature. First, some authors described the evolution of Young's modulus. Different methods were proposed, for example the entropy spring theory (Wang et al., 2008) or the molecular dynamic approach (Ding et al., 2012). Second, some tried to describe non-linear elasticity, i.e. hyperelasticity. In this way, Soares introduced a degradation damage parameter in classical hyperelastic models. The same approach can be used with viscoelastic models. Soares introduced a degradation parameter in Quasi-Linear Viscoelastic and in Pipkin and Rogers (1968) model. His degradation variable approach was then the commonly used formalism in hydrolytic degradable mechanical model. Muliana and Rajagopal (2012) introduced also a strain and water concentration dependance of the hydrolytic damage parameter in the modelling but few experimental tests were used to validate the model along the degradation process. Finally, Vieira et al. (2014) used a non-linear viscoelastic model, the Bergström and Boyce (1998) model to describe PLA-PCL fibers but the authors only present loading curves in their paper to model loss of mechanical properties.

The objective of this paper is to characterize an amorphous bioresorbable PLA-*b*-PEG-*b*-PLA triblock copolymer and to model its mechanical behaviour during degradation. At first, different physical properties like mass and molecular weight of the polymer are presented for different steps of degradation. Then, loss of mechanical properties is studied from uniaxial load and relaxation tests, performed in an aqueous media at 37 °C. From the relaxation curves, a linear viscoelastic model based on a hydrolytic damage variable is developed and compared to experimental data. The abilities of the modelling are finally analysed.

2. Materials and methods

2.1. Material

Poly(ethylene glycol) (average M_n 20 000 g/mol), tin(II) 2-ethylhexanoate (Sn(Oct)2, 95%), dichloromethane (DCM), diethyl ether and tetrahydrofuran (THF) were purchased from Sigma-Aldrich (St-Quentin Fallavier, France). D,L-lactide (D,L-LA) was purchased from Purac (Lyon, France).

2.2. Analysis

^{1}H NMR spectra were recorded at room temperature using an AMX300 Bruker spectrometer operating at 300 MHz. Deuterated chloroform was used as solvent, chemical shifts were expressed in ppm with respect to tetramethylsilane (TMS).

Number average molecular weight (M_n) and polydispersity (PD) of the polymers were determined by size exclusion chromatography (SEC) using a Viscotek GPCMax autosampler system fitted two Viscotek LT5000L Mixed Medium columns (300 × 7.8 mm), a Viscotek VE 3580 RI detector. The mobile phase was THF at 1 mL/min flow and 30 °C. Typically, the polymer (20 mg) was dissolved in THF (2 mL) and the resulting solution was filtered through a 0.45 μm Millipore filter before injection of 20 μL of filtered solution. M_n was expressed according to calibration using Polystyrene standards.

For mass loss measurement, films of 20 mm long, 10 mm and 0.5 mm thick were prepared. They were then placed in 20 mL test tubes and submitted to different times of degradation between 0 and 12 weeks in phosphate buffer solution (PBS) at 37 °C within an agitator/incubator. The initial mass (m_0) was measured in the initial state. At a given step of degradation, films were taken out of the solution, dried and weighted again to obtain the dry mass (m_d). Mass loss was then calculated with the following equation:

$$M_{loss}(\%) = 100 \times \frac{m_0 - m_d}{m_0}$$

For every property measured, 3 samples were tested. The standard deviations were calculated and indicated on the curves by error bars.

2.3. Copolymers synthesis

PLA50-b-PEG-b-PLA50 triblock copolymer was synthesized following a procedure previously described by Leroy et al. (2013). Typically, predetermined amounts of D,L-LA and PEG were introduced in a flask. Sn(Oct)2 (0.1 molar % with respect to LA units) was then added. After degassing, the flask was sealed under vacuum and polymerization was allowed to proceed at 110 °C. After 5 days, the copolymer was recovered by dissolution in DCM and precipitation in cold diethyl ether. Finally, the product was dried under reduced pressure to constant mass. The copolymer was obtained with a yield of 90%.

Polymerization degree of each PLA block and molecular weight of the synthesized triblock copolymers were calculated using Eqs. (1) and (2) respectively:

$$DP_{PLA}(\%) = \frac{1}{2} \times \frac{DP_{PEG}}{\frac{EG}{LA}} \quad (1)$$

$$M_{ntribloc}(\%) = 2 \times (DP_{PLA} \times 72) + M_{nPEG} \quad (2)$$

with *EG/LA* being the ratio of ethylene oxide and lactyl units calculated from ^{1}H NMR spectra.

^{1}H NMR: (300 MHz; CDCl3): δ (ppm)=5.1 (q, 1H, CO-CH (CH3)-O), 3.6 (s, 4H, CH2-CH2-O), 1.5 (m, 3H, CO-CH(CH3)-O). $M_{ntribloc}$=345 000 g/mol, *LA/EG*=10/1.

The polymer films were manufactured by solvent evaporation. A predefined quantity of polymer was solubilized in acetone, spread in a small dish and placed for 36 h under an extractor hood for evaporation. Final solvent removal was obtained by further drying in *vacuo* under $1 \cdot 10^{-3}$ mBar for 3 days. A 0.5 mm thick film was then obtained.

2.4. Methods for mechanical properties measurement

The mechanical tests were realized with dogbone tensile specimens of 14 mm in length and 3 mm wide gauge length cut in the films with a specific punch and put in degradation with the same method as the one described previously. At least two specimens were used for each test. PLA-*b*-PEG-*b*-PLA is an hydrophilic thermoplastic polymer. Thus, it is very sensitive during mechanical tests to environmental conditions. An experimental set-up to make mechanical immersed tests at controlled temperature of 37 °C was designed and is presented in Fig. 1. It consists in a steel hermetic bath adjustable on the mechanical test machine. The heating of the liquid is made by heat cartridges inserted in specific sites under the bath. Temperature regulation is assured by a proportional-integral-derivative controller system linked to a resistance temperature detectors probe that controls electrical power send to cartridges.

The mechanical tests consist in a load at two strain levels (2% and 4%) with a strain rate during loading of 1% per second followed by a tensile relaxation test. Mechanical tests were realized with a Gabo Eplexor mechanical test machine with a load cell of 10 N at 0, 1, 3, 5 and 7 weeks of degradation.

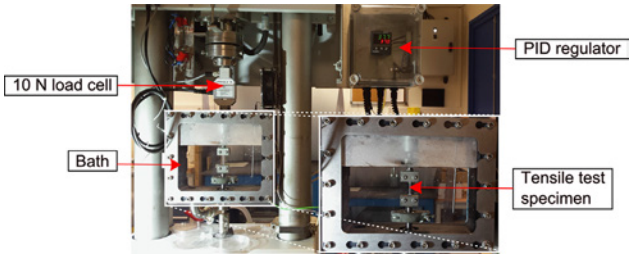

Fig. 1 – Experimental set up for mechanical immersed tests.

To measure the strain field, a Vic 2D image correlation software is used. During mechanical tests, images of the specimens are recorded with a camera at a frequency of 30 Hz. Digital image correlation (DIC) consists in an optical method that employs tracking of speckle points between different images to rebuild a local strain field. Beyond 7 weeks, the loss of mechanical properties of the specimen are too important to be tested.

3. Results and discussions

3.1. Physical properties evolution

The mass loss is presented in Fig. 2. It gives information about water soluble oligomers generated by the hydrolysis process and released out of the polymeric structure. Two distinctive periods are observed. During the three first weeks, the mass loss rate is relatively weak (about 3% per week) compared to the following weeks (about 10% per week). This induction period is commonly observed during the degradation of aliphatic polyesters and is due to the difficulty, At first, for the degraded chains to diffuse out of the sample (Leroy et al., 2013; Li et al., 1990). After this period, the density of chains starts to decrease and the products of degradation can be released in the media, the weight is decreasing almost linearly.

The normalized number average molecular weight defined as number average molecular weight (M_n) divided by the initial number average molecular weight (M_{n0}) is shown in Fig. 3. Unlike mass loss, the decrease is very important during the two fist weeks. Indeed, about 60% of the initial molar mass is lost during this period. This trend is explained by the highest concentration of ester bonds per volume unit leading to a greater ability of long chains to be hydrolysed (Wang et al., 2008). In the latter stages, concentration of ester bonds is very low, making scission probability and hydrolysis rate almost non-existent. Dispersity index presented in Fig. 3 is defined as the ratio of the mass average molecular weight and the number average molecular weight and describes the degree of "non-uniformity" of a chain distribution. The increase of dispersity index appears in parallel with the decrease of molecular weight. These results highlight the rise of dispersion of chain lengths due to the random break of chains that occurs during the degradation process.

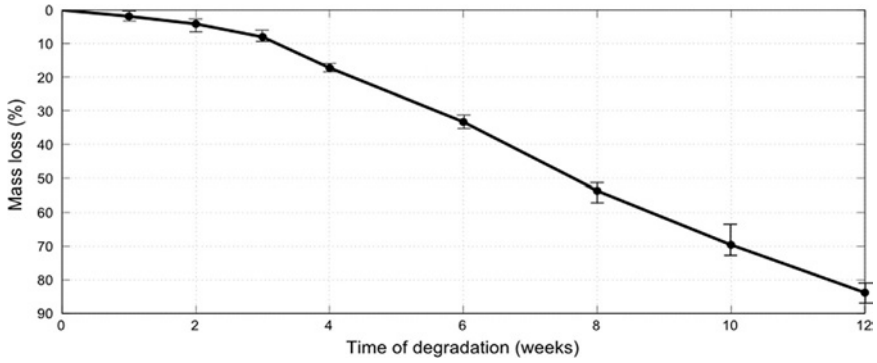

Fig. 2 – Normalized weight loss of PLA-*b*-PEG-*b*-PLA triblock copolymer during 12 weeks of degradation in PBS at 37 °C.

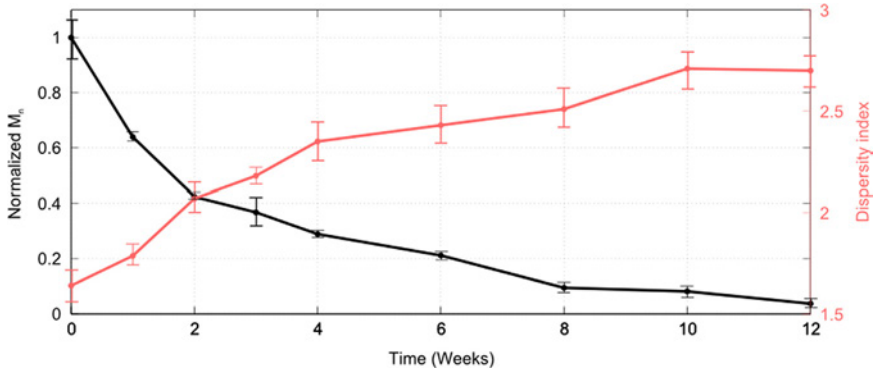

Fig. 3 – Number average molecular weight and dispersity index evolution of PLA-*b*-PEG-*b*-PLA triblock copolymer during 12 weeks of degradation in PBS at 37 °C.

3.2. *Mechanical properties evolution*

The mechanical properties were tested between zero and seven weeks. As seen previously (cf. Fig. 3), after eight weeks, the polymer has lost almost 90% of its initial molecular weight, making mechanical tests impossible due to the extreme brittleness of the specimens. Fig. 4 presents the stress–strain curves of the material for the tensile test at a strain of 4%. In the non-degraded state, stress is increasing between 0 and 2% before reaching a plateau. The maximum stress level observed is 2.7 MPa. In the course of degradation, the long polymeric chains are cleaved, leading to a decrease of molecular weight and mechanical properties. Even if the shape of the non-degraded curve is conserved, the maximal stress decreases. 15% of the initial stress is lost after 3 weeks and 50% after 5 weeks. Figs. 5 and 6 present load–relaxation tests at a strain of 2% and 4% respectively. In this last figure, the load part corresponds to Fig. 4. Actually, when strain is maintained after loads, a stress relaxation is measured, illustrating the viscoelastic behaviour of the material. Stress fell of about 90% during the first 10 s and reaches nearly zero after 30 s. This means that relaxation times are very short.

In order to compare the relaxation after the different degradation times, the normalized relaxation is used. It consists in the ratio of the current stress to the static stress before relaxation. If σ_m is the static stress reached at the end of the load (corresponding to the dotted vertical lines in Figs. 5 and 6) and σ_{relax} the stress recorded during relaxation, the equation of the normalized relaxation is:

$$\sigma_{nr} = \frac{\sigma_{relax}}{\sigma_m} = \frac{\sigma_{relax}}{\sigma_{relax}(t=0)} \tag{3}$$

In this last equation, t represents the time recorded during the stress relaxation. Thus, the initial time corresponds to the end of the load (represented by the dotted vertical lines in Figs. 5 and 6). The curves for relaxation at 2% and 4% are represented in Figs. 7 and 8. The curves are nearly similar during the 5 first weeks of degradation for the two values of maximal strain. In other words, it means that the temporal viscous component of the mechanical behaviour is invariant during early stages of degradation. This means that, during this period, only instantaneous elastic properties degrades. From week 7 results, some changes in the normalized relaxation curves are observed. Relative stress decreases faster at the beginning of the relaxation with a dramatical fall in the first instants after the end of the load. This implies that viscous properties only start to change after reaching late stages of degradation.

4. Consitutive modelling: a linear viscoelastic degradable model

The aim of this section is to develop a simple viscoelastic model that takes into account the evolution of mechanical properties during degradation. At first, a linear viscoelastic model is chosen

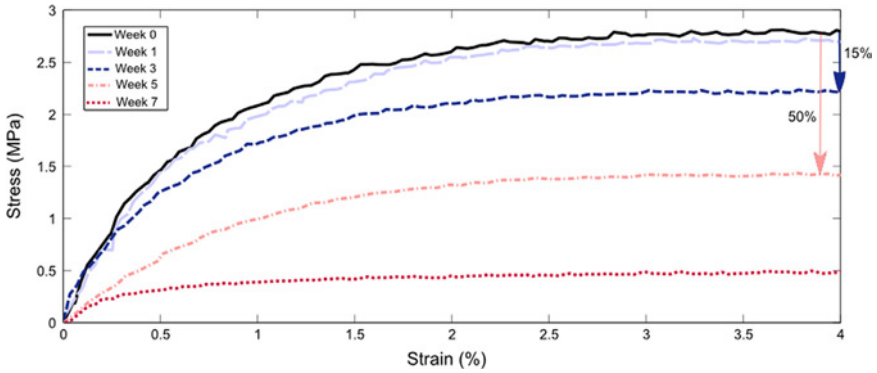

Fig. 4 – Load part of the relaxation test at 4% strain load at 0, 1, 3, 5 and 7 weeks of degradation.

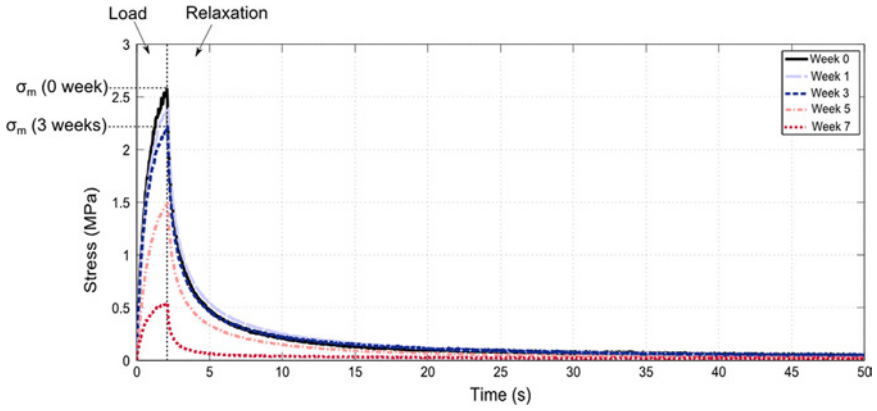

Fig. 5 – Relaxation tests at 2% strain load at 0, 1, 3, 5 and 7 weeks of degradation.

to model the non-degraded material behaviour. Then, based on the use of an hydrolytic damage variable, this model will be adapted in order to consider the loss of mechanical properties.

4.1. *Hypothesis*

It is considered that the polymer is sufficiently hydrophilic to present a bulk erosion scheme and sufficiently thin to neglect autocatalytic effects (Grizzi et al., 1995). Thus, the strain and degradation states are identical in every point of the specimens.

4.2. *Linear viscoelastic model*

To model the mechanical behaviour of the material, a hereditary integral representation of stress and strain is used. It is based on Boltzmann's superposition principle. At first, the uniaxial representation of the stress–strain constitutive relation is considered:

$$\sigma(t) = \int_0^t E(t-\tau)\frac{d\varepsilon}{d\tau}\,d\tau \tag{4}$$

where E is the stress relaxation modulus, σ is the Cauchy stress and ε is the strain. This equation is classically used to describe linear viscoelastic behaviour in small strain. To model the mechanical behaviour of the polymer, a simple generalized Maxwell model with n branches is used. The corresponding rheological model is presented in Fig. 9.

In the generalized Maxwell model, the normalized relaxation curve takes the form of a Prony's series:

$$\sigma_{nr} = \frac{\sigma_{relax}}{\sigma_{relax}(t=0)} = a_0 + \sum_{i=1}^{n} a_i e^{-\frac{t}{\tau_i}} \tag{5}$$

a_i are the amplitudes of Prony's series and τ_i are the characteristic relaxation times. The first step of the calibration of the model consists in fitting the normalized relaxation curve for the non-degraded material. The relaxation curve is fitted for different number of terms in Prony's series until finding the minimal number of terms that fits well the curve. The parameters are listed in Table 1. Fig. 10 presents the fits for different number of parameters. The use of one or two parameters does not allow us to model every characteristic times of relaxation, at least three terms are required. The same results are obtained at 4% but the curves are not presented here.

The results highlight that three Prony's series terms must be used to model the relaxation curve representing seven parameters: $a_0, a_1, a_2, a_3, \tau_1, \tau_2, \tau_3$. In this way, the hereditary integral model of Eq. (4) becomes:

$$\sigma(t) = \int_0^t \left(E_0 + \sum_{i=1}^{3} E_i e^{-\frac{t-\tau}{\tau_i}}\frac{d\varepsilon}{d\tau}\right) d\tau \tag{6}$$

The E_i terms are the amplitudes of the viscoelastic model. From the equation of the normalized relaxation curve (Eq. (5)), the real relaxation curve equation can be rebuilt from the a_i values and deduced from Eq. (6):

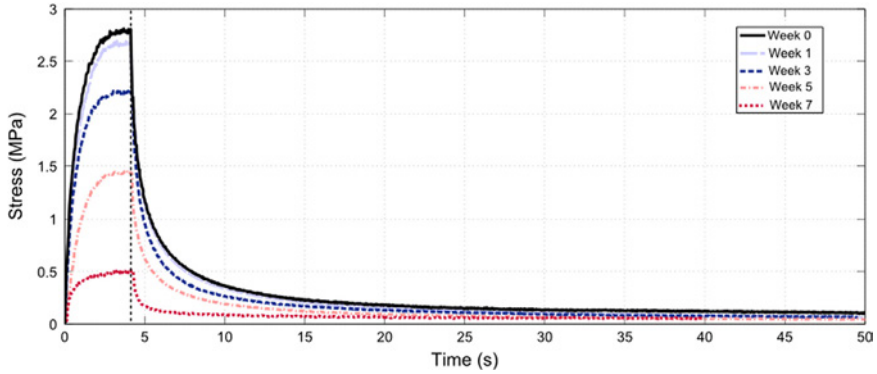

Fig. 6 – Relaxation tests at 4% strain load at 0, 1, 3, 5 and 7 weeks of degradation.

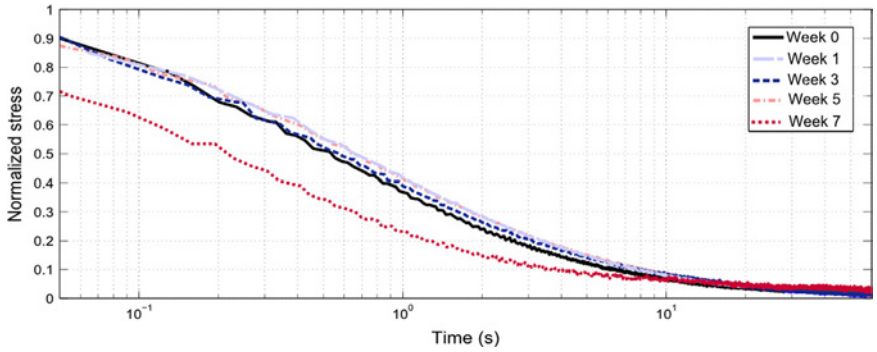

Fig. 7 – Normalized relaxation curves at 2% strain load at 0, 1, 3, 5 and 7 weeks of degradation.

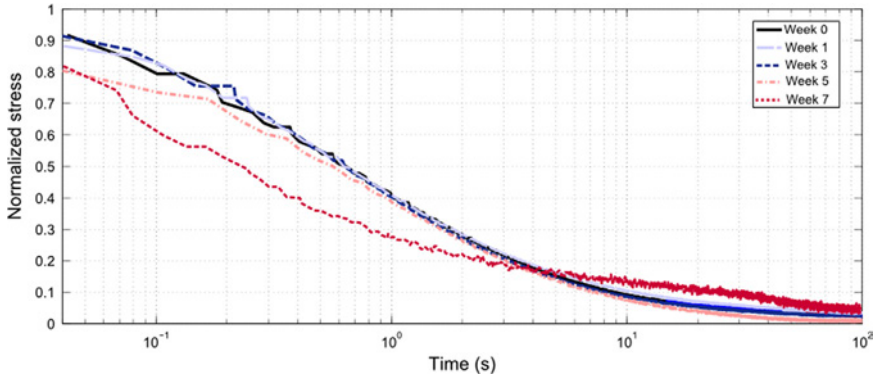

Fig. 8 – Normalized relaxation curves at 4% strain load at 0, 1, 3, 5 and 7 weeks of degradation.

$$\sigma_{relax}(t) = \left(E_0 T + \sum_{i=1}^{3} E_i \tau_i \left(e^{\frac{T}{\tau_i}} - 1 \right) e^{-\frac{t}{\tau_i}} \right) \frac{d\varepsilon}{d\tau} \tag{7}$$

where T represents here the duration of the load. The values of E_i can be determined from the values of a_i by identification of the amplitudes coefficients. The relevance of the model to describe the non-degraded state is then estimated from the comparison between experimental load stress–strain curves and the model. The model perfectly matches the experimental load curve for the 2% strain in the non-degraded state as can be seen in Fig. 13(a).

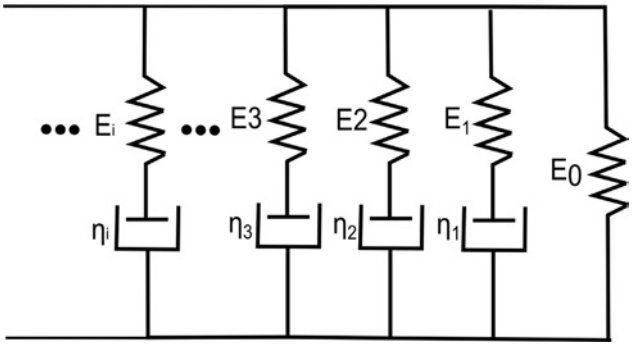

Fig. 9 – Rheological scheme of the linear viscoelastic model.

Table 1 – Values of the different parameters of the model.

Strain (%)	a_0	a_1	a_2	a_3	E_0 (MPa)	E_1 (MPa)	E_2 (MPa)	E_3 (MPa)	τ_1 (s)	τ_2 (s)	τ_3 (s)
2	0.01	0.27	0.45	0.27	1.3	40.9	146.9	470.3	6.3	0.92	0.15
4	0.04	0.2	0.49	0.26	3	17.9	131.6	504.9	7.17	1.07	0.14

Exp. model a	Exp. model b	Lin. model c	K (1/week)
5.75	10.55	0.20	0.623
3.9	8.28	0.27	0.623

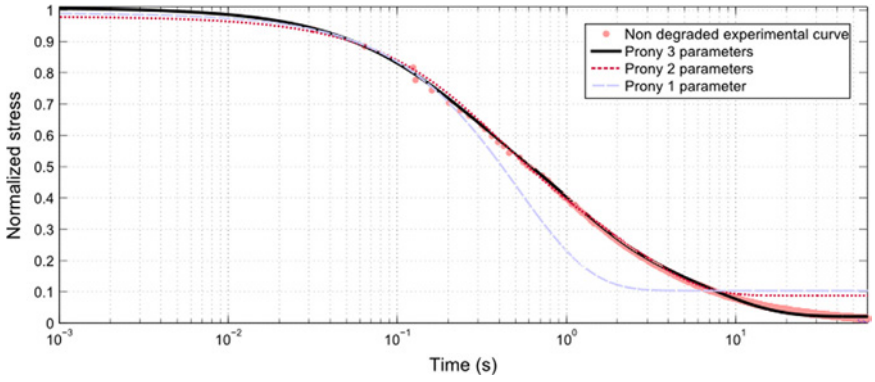

Fig. 10 – Relaxation curves fitting for different numbers of terms in Prony series.

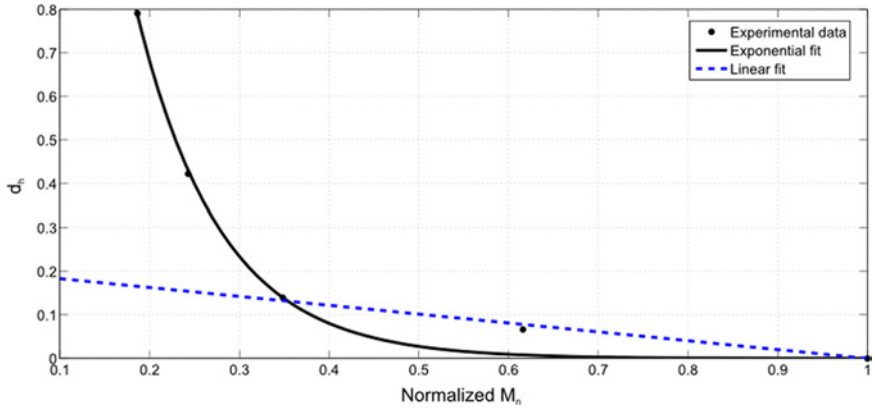

Fig. 11 – Degradation parameter's evolution fitting during the 7 first weeks of degradation.

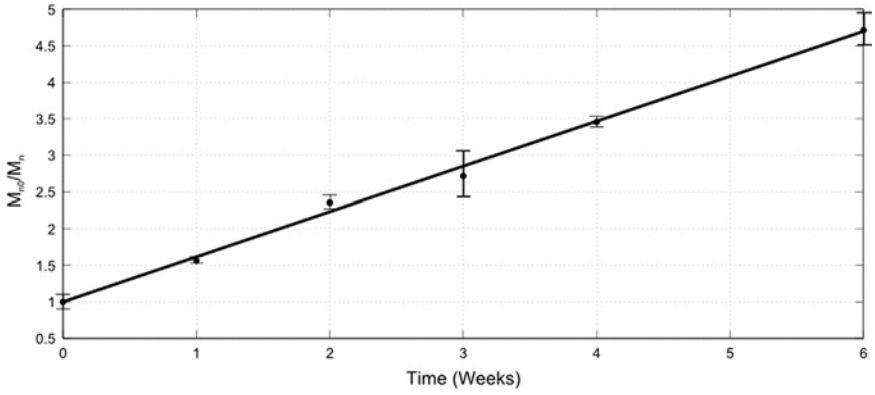

Fig. 12 – Number average molecular weight evolution fitting during the 7 first weeks of degradation.

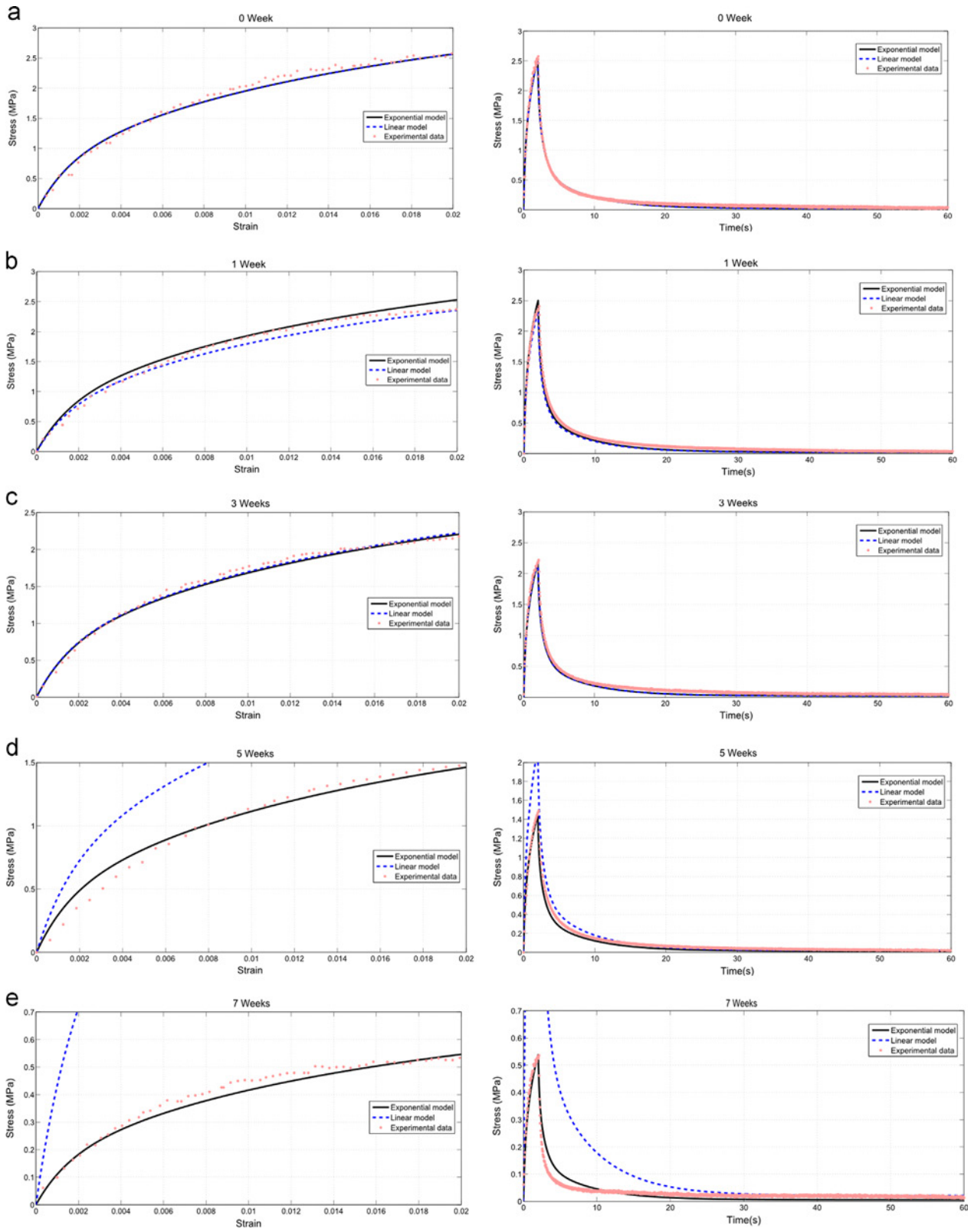

Fig. 13 – Axial nominal stress vs. nominal strain and load-relaxation curves for 0, 1, 3, 5 and 7 weeks of degradation with corresponding calibrated linear viscoelastic material model on the 2% load strain curves for the 2% strain's test.

To take into account the evolution of mechanical properties during degradation, a scalar parameter $d_h(\mathbf{x}, t)$ is introduced. It represents the degraded state of the polymer at each material point $\mathbf{x}$ and at a given time t (Soares et al., 2008). As seen in the hypothesis in Section 4.1, d_h is supposed independent of the location in the specimen. d_h has a value

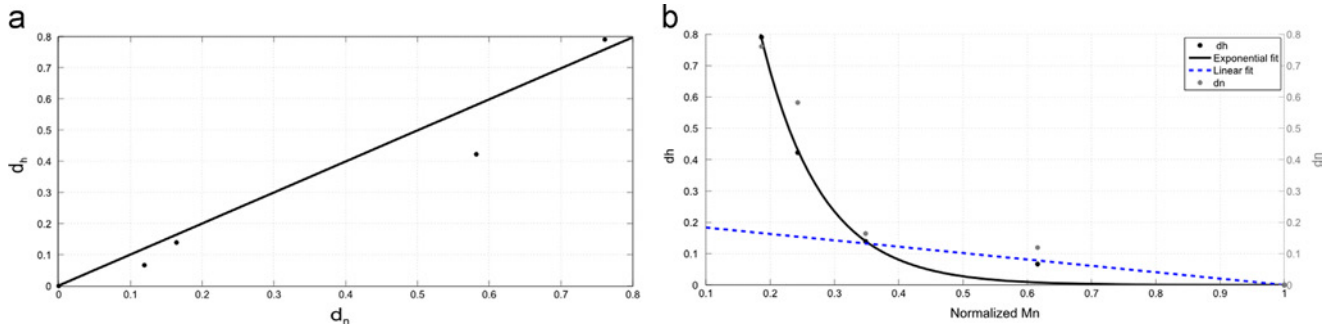

Fig. 14 – (a) Hydrolytic damage parameter vs. chain density damage parameter. (b) Evolution of hydrolytic damage parameter and chain density damage parameter as a function of normalized number average molecular weight.

between 0 and 1, 0 representing a non-degraded state and 1 a fully degraded state. As highlighted by the results in Section 3.2, the relaxation can be considered as independent of the degradation time, it means that only the elastic part of the model is concerned by the degradation:

$$\sigma_{relax}(d_h,t)=\frac{\sigma_{relax}(d_h,0)}{\sigma_{relax}(d_h=0,0)}\times\sigma_{relax}(d_h=0,t) \tag{8}$$

From Eq. (7), the general following equation can be obtained:

$$\sigma_{relax}(d_h,t)=E_0T\times\frac{\sigma_{relax}(d_h,0)}{\sigma_{relax}(d_h=0,0)}+\sum_{i=1}^{3}E_i\frac{\sigma_{relax}(d_h,0)}{\sigma_{relax}(d_h=0,0)}\left(\tau_i\left(e^{\frac{T}{\tau_i}}-1\right)e^{-\frac{t}{\tau_i}}\right)\frac{d\varepsilon}{d\tau} \tag{9}$$

From the definition of Lemaitre and Chaboche (1985) used by Vieira et al. (2011) for hydrolytic damage, the degradation variable is defined as:

$$d_h=1-\frac{\sigma_m(d_h)}{\sigma_m(d_h=0)}=1-\frac{\sigma_{relax}(d_h,0)}{\sigma_{relax}(d_h=0,0)} \tag{10}$$

$\sigma_m(d_h)$ is the maximum stress reached at the end of the load for a given degradation state d_h and corresponds to the time zero of the relaxation (5). Consequently, the stress can be expressed as:

$$\sigma_{relax}(d_h,t)=\left(E_0T\times\frac{\sigma_{relax}(d_h,0)}{\sigma_{relax}(d_h=0,0)}+\sum_{i=1}^{3}E_i\frac{\sigma_{relax}(d_h,0)}{\sigma_{relax}(d_h=0,0)}\,\tau_i\left(e^{\frac{T}{\tau_i}}-1\right)e^{-\frac{t}{\tau_i}}\right)\frac{d\varepsilon}{d\tau} \tag{11}$$

$$\sigma_{relax}(d_h,t)=\quad E_0T\times(1-d_h)+\sum_{i=1}^{3}E_i\times(1-d_h)\,\tau_i\left(e^{\frac{T}{\tau_i}}-1\right)e^{-\frac{t}{\tau_i}}\Bigg)\frac{d\varepsilon}{d\tau} \tag{12}$$

Finally, the degradation evolution must be determined. As explained in the introduction, when water diffuses into the polymeric structure, hydrolysis reaction breaks the ester links leading to the chains cleavage. This leads to the creation of oligomers and monomers. The main consequence is the decrease of the number average molecular weight (accompanied by a loss of mechanical properties). Thus, the parameter chosen to describe the mechanical behaviour evolution is number average molecular weight. Pan and Chen (2015) developed a basic model for the evaluation of number average molecular weight during degradation for amorphous biodegradable polymer. They showed that, in the absence of autocatalytic effect, molecular weight M_n, in early stages of degradation, can take the form:

$$\frac{M_{n0}}{M_n}=1+Kt \tag{13}$$

where K is a parameter that is proportional to the hydrolysis rate. This function is fitted on experimental data and presented in Fig. 12 and the value of the parameter is presented in Table 1. The figure shows that the fit is adapted to describe the evolution of the number average molecular weight.

The degradation parameter (Eq. (10)) depends on the relaxation curve. In a first step, the 2% strain data are considered. In Fig. 11, d_h is plotted as a function of the normalized number average molecular weight (the same analysis was realized for the 4% strain data but is not presented here).

For weak degradation time, the data present a quite linear part, until a normalized M_n value of 0.35 corresponding to three weeks. A linear form of the damage parameter is proposed as:

$$d_h=c\times\left(1-\frac{M_n}{M_{n0}}\right) \tag{14}$$

where c is a material parameter. Nevertheless, this model cannot describe the strong damage between the third and the seventh week (cf. Fig. 11). In this case, an exponential form is proposed as:

$$d_h=a\times e^{-b\times\frac{M_n}{M_{n0}}} \tag{15}$$

where a and b are material parameters. The material parameters are fitted for 2% and 4% strain relaxation curves and the values of the parameters are presented in Table 1.

It must be noticed that this equation for d_h evolution is only valid for the 7 first weeks during which mechanical properties are measurable. It is obvious that the structure is fully degraded many weeks after total loss of mechanical properties.

In Fig. 13, the model calibrated from the 2% load relaxation curve is compared to experimental data. The linear form of the degradation model is able to describe the evolution of the mechanical properties during the three first weeks of degradation but fails to model the advanced degradation states as expected by the fit of the damage variable (cf. Fig. 11). In the case of the exponential model, the results are very good for every steps of degradation, even in the most degraded case. Only the relaxation curve at seven weeks is not perfectly well

fitted. This result was expected and is due to the evolution of viscoelastic properties in latter stages of degradation that is not taken into account (cf. Figs. 7 and 8). The advantage of this approach is that a very simple and easy to calibrate model is obtained. It provides tools to simulate the viscoelastic behaviour's evolution during degradation for small strain loaded structures. The model calibrated from 2% load relaxation is used to simulate the relaxation at 4%, the results are presented in Fig. 15. First, by analyzing the loading curves, it appears that the model fails to describe the stress plateau that appears between 2% and 4%. Indeed, the stress in the model still increases beyond 2% strain when it remains constant in the experimental load curve, overestimating the maximum stress. Moreover, for the viscoelastic part, during the 3 first weeks of degradation, the model underestimates the residual stress that remains at the end of the relaxation.

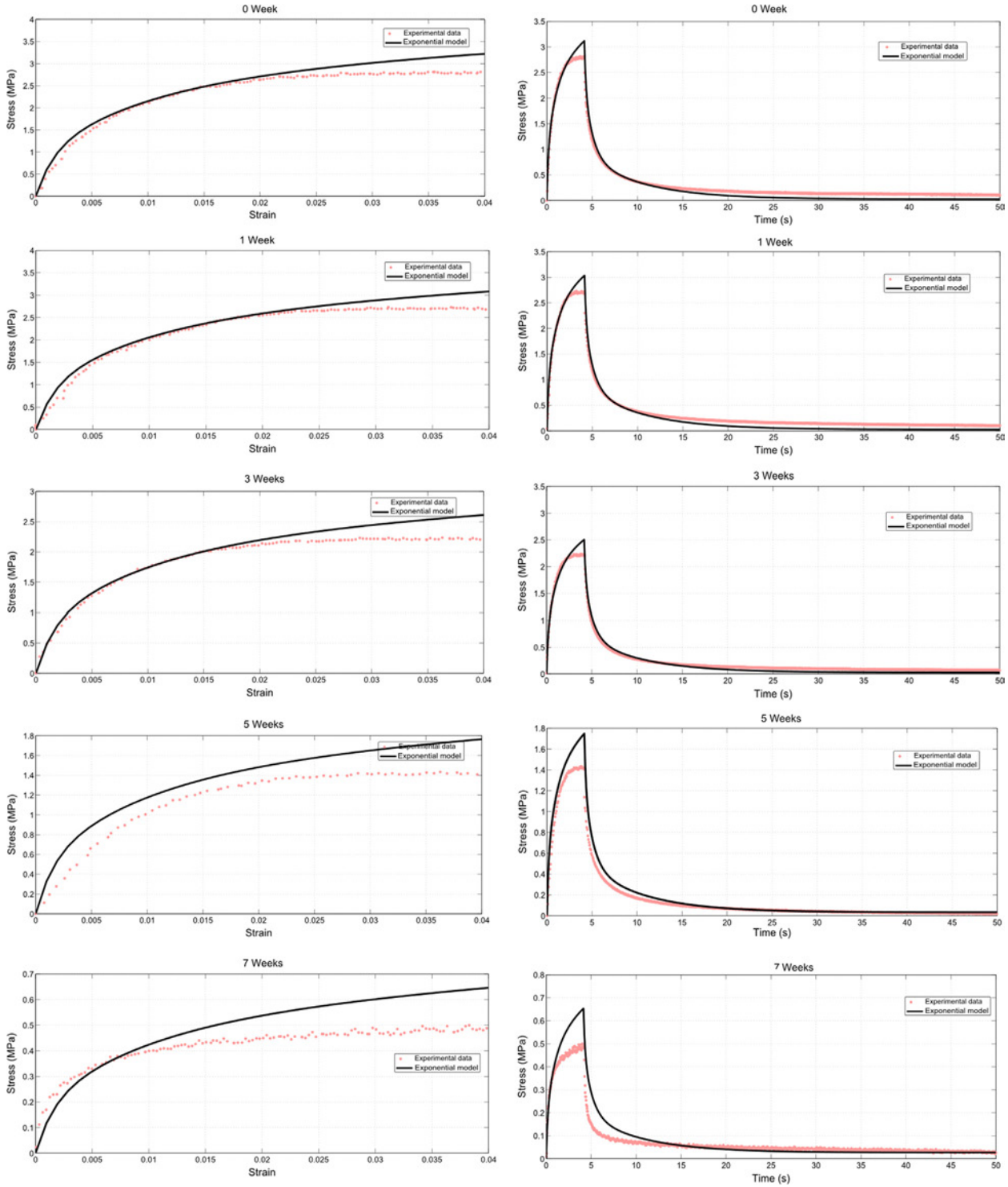

Fig. 15 – Axial nominal stress vs. nominal strain and load-relaxation curves for 0, 1, 3, 5 and 7 weeks of degradation with corresponding calibrated linear viscoelastic material model on the 2% load strain curves for the 4% strain's test.

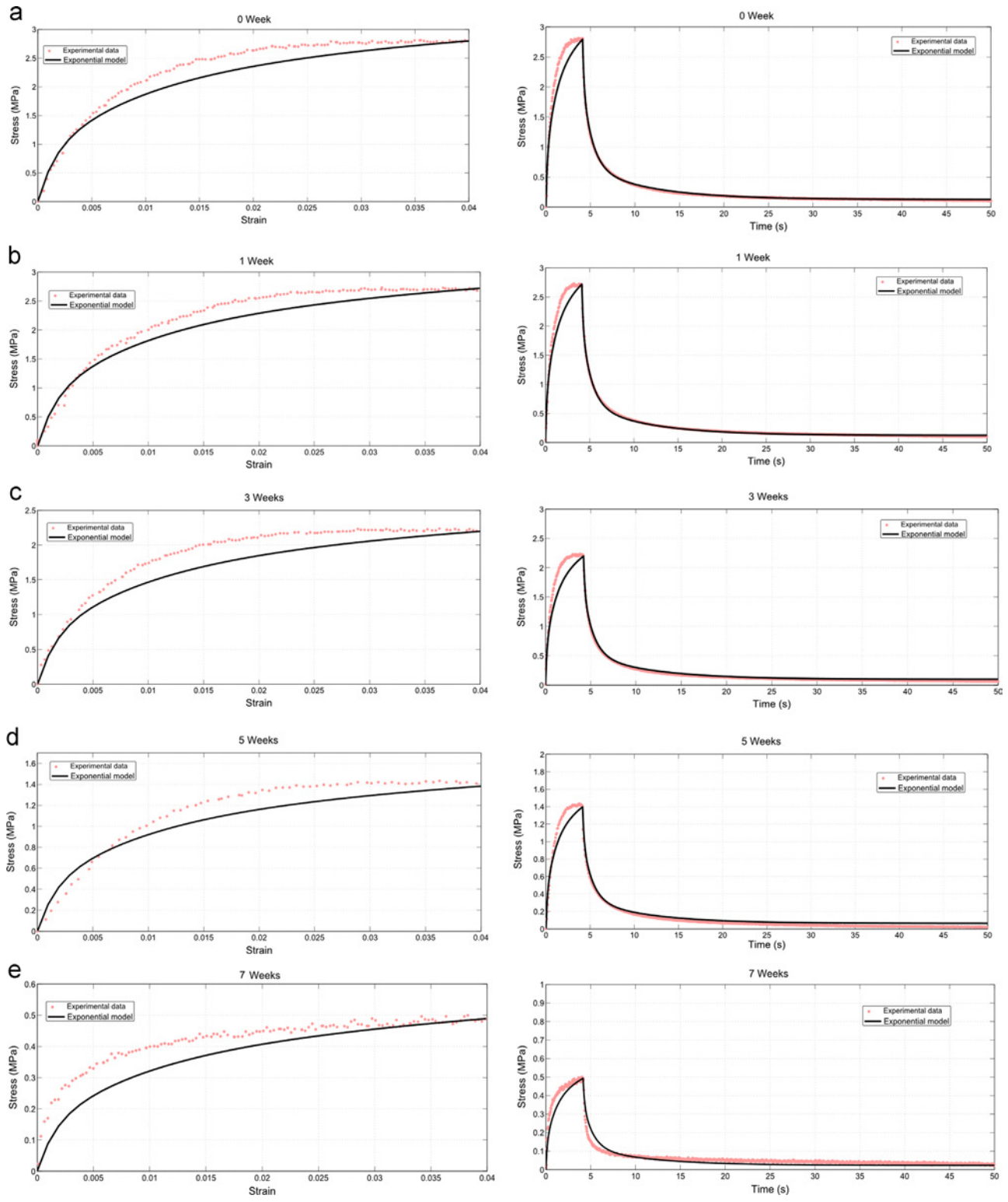

Fig. 16 – Axial nominal stress vs. nominal strain and load-relaxation curves for 0, 1, 3, 5 and 7 weeks of degradation with corresponding calibrated linear viscoelastic material model on the 4% load strain curves for the 4% strain's test.

Table 2 – Values of the Neo-Hookean hyperelastic coefficients for the different steps of degradation.

	0 week	1 week	3 weeks	5 weeks	7 weeks
nkT (MPa)	67	59	54	28	16

The model fails to predict deformation larger from the fitted ones. Finally, it was fitted directly on 4% curves, the material parameters are presented in Table 1 and the results are presented in Fig. 16. Indeed, the model curves remain monotonically increasing and still does not model the plateau. The maximum stress is well estimated but the stress is underestimated between 0.5% and 4% during the loading. At week 7, the stress is underestimated for the whole load curve and overestimated for the beginning of the relaxation. These are the limits of the linear viscoelastic approach. The linear viscoelasticity cannot describe a too long plateau. Nevertheless, this approach succeed to describe moderate strains with a model that is very easy to fit. It only needs to have a monotonic strain–stress curve for the different degradation times and a normalized relaxation curve as it was shown that this curve is independent of the degradation time for the PLA-*b*-PEG-*b*-PLA.

4.3. *Initial strain–stress curve analysis*

The initial stiffness of the curve is analysed by fitting the first part of the load strain–stress curves on the 2% maximal strain curves with a simple Neo-Hookean model (Treloar, 1943) i.e. for strain lower than 0.3%. The material parameters nkT are fitted for every steps of degradation and presented in Table 2. From the statistical theory of elasticity, the volumic density of chains n can be deduced as k is the Boltzmann constant and T is the temperature.

During degradation, the hydrolysis process breaks the ester links leading to a decrease of the chain's density. One of the main consequences is the decrease of the elastic modulus. The damage of the initial stiffness can be evaluated with the ratio of the chain density for a virgin material and for a degraded one. By analogy with the hydrolytic damage parameter, a density of chains damage parameter can be defined as:

$$d_n = c \times \left(1 - \frac{n}{n_0}\right) \tag{16}$$

n_0 is the initial chain density. In Fig. 14(a), the hydrolytic damage parameter is plotted as a function of the chain density damage parameter. As expected from the comparison between experimental data and the previously fitted model (cf. Fig. 13), the two parameters are quasi-similar except for the fifth week of degradation. As it can be observed in Fig. 13(d), the model overestimates the initial stiffness for this state of degradation. Then, the two damage parameters are plotted in function of the normalized M_n in Fig. 14(b). As noticed previously, the values of the two damage parameters are close except in the case of the week 5 of degradation. Despite the weak difference between d_n and d_h, a very good approximation can be obtained with the initial modulus, proving that the model can also be calibrated only with the initial stiffness of the material.

5. Conclusions

In this paper, a complete study was realized on a PLA-*b*-PEG-*b*-PLA triblock copolymer during in vitro degradation. After measuring the different material's physical properties such as mass loss, number average molecular weight and dispersity index, a mechanical study was made. The experimental protocol consisted in realizing load and relaxation stress tests, in a controlled environment similar as the in vivo one, for different degradation times. A loss of mechanical properties has been observed, particularly the maximum stress reached at the end of the load. A master curve was obtained for relaxation behaviour. This leads us to consider that only the elasticity of the material was alterated in the first weeks. A linear viscoelastic model was used to model the mechanical behaviour of the material in the non-degraded state. Then, based on a degradation variable and on the invariance of normalized relaxation curve during degradation, the model was adapted to take into account the evolution of mechanical properties. The degradation variable was linked to number average molar mass in order to determine its complete kinetic over time. It was shown that the model fits very well the stress–strain curve for strains smaller than 2% for all degradation steps. For weak deformations, the model can also be calibrated by means of the fit of the initial stiffness of the material. However, it is unable to predict the mechanical behaviour for upper deformations. The linear elasticity is not able to describe a stress plateau, meaning that other modelling approaches should be used to describe the elasticity of the material. Finally, the results highlight that only one relaxation test and a monotonic tensile for each degradation times are needed to perfectly fit the model parameters.

REFERENCES

Bergström, J.S., Boyce, M.C., 1998. Constitutive modeling of the large strain time-dependent behavior of elastomers. J. Mech. Phys. Solids 46 (5), 931–954.

Chen, Q., Liang, S., Thouas, G.A., 2013. Elastomeric biomaterials for tissue engineering. Prog. Polym. Sci. 38 (3–4), 584–671.

Ding, L., Davidchack, R.L., Pan., J., 2012. A molecular dynamics study of Young's modulus change of semi-crystalline polymers during degradation by chain scissions. J. Mech. Behav. Biomed. Mater. 5 (1), 224–230.

Göpferich, A., 1996. Mechanisms of polymer degradation and erosion. Biomaterials 17 (2), 103–114.

Garric, X., Guillaume, O., Dabboue, H., Vert, M., Molès, J.P., 2012. Potential of a PLA-PEO-PLA-based scaffold for skin tissue engineering: in vitro evaluation. J. Biomater. Sci. Polym. Ed. 23 (13), 1687–1700.

Grizzi, I., Garreau, H., Li, S., Vert, M., 1995. Hydrolytic degradation of devices based on poly(DL-lactic acid) size-dependence. Biomaterials 16 (March (4)), 305–311.

Ikada, Y., Tsuji, H., 2000. Biodegradable polyesters for medical and ecological applications. Macromol. Rapid Commun. 21 (3), 117–132.

Karjalainen, T., Hiljanen-Vainio, M., Malin, M., Seppala, J., 1996. Biodegradable lactone copolymers. III. Mechanical properties of c-paprolactone and lactide copolymers after hydrolysis in vitro. J. Appl. Polym. Sci. 59 (8), 1299–1304.

Lemaitre, J., Chaboche, J.-L., 1985. Mécanique des Matériaux Solides. Dunod, Paris.

Leroy, A., Pinese, C., Bony, C., Garric, X., Noël, D., Nottelet, B., Coudane, J., 2013. Investigation on the properties of linear PLA-poloxamer and star PLA-poloxamine copolymers for temporary biomedical applications. Mater. Sci. Eng. C—Mater. Biol. Appl. 33 (7), 4133–4139.

Li, S., Garreau, H., Vert, M., 1990. Structure-property relationships in the case of the degradation of massive poly (-hydroxy acids)

in aqueous media Influence of the morphology of poly (L-/actic acid). J. Mater. Sci.: Mater. Med. 1 (4), 198–206.
Maurus, P.B., Kaeding, C.C., 2004. Bioabsorbable implant material review. Oper. Tech. Sports Med. 12 (3), 158–160.
Muliana, A., Rajagopal, K.R., 2012. Modeling the response of nonlinear viscoelastic biodegradable polymeric stents. Int. J. Solids Struct. 49 (7–8), 989–1000.
Nair, L.S., Laurencin, C.T., 2007. Biodegradable polymers as biomaterials. Prog. Polym. Sci. 32 (8–9), 762–798.
Pan, J., Chen, X., 2015. Modelling degradation of amorphous biodegradable polyesters: basic model. In: Pan, J. (Ed.), Modelling Degradation of Bioresorbable Polymeric Medical Devices. Woodhead Publishing Series in Biomaterials. Woodhead Publishing, Cambridge, pp. 15–31.
Park, H., Park, K., Waleed, S.W.S., 2011. Biodegradable hydrogels for drug delivery. CRC Press, Lancaster.
Perego, G., Cella, G.D., Bastioli, C., 1998. Effect of molecular weight and crystallinity on poly(lactic acid) mechanical properties. J. Appl. Polym. Sci. 59 (1), 37–43.
Pipkin, A.C., Rogers, T.G., 1968. A non-linear integral representation for viscoelastic behaviour. J. Mech. Phys. Solids 16 (1), 59–72.
Soares, J.S., Moore Jr., James E., Rajagopal, K.R., 2008. Constitutive framework for biodegradable polymers with applications to biodegradable stents. Asaio J. 54 (3), 295–301.
Stefani, M., Coudane, J., Vert, M., 2006. In vitro ageing and degradation of PEG-PLA diblock copolymer-based nanoparticles. Polym. Degrad. Stab. 91 (11), 2554–2559.
Tessmar, J.K., Göpferich, A.M., 2007. Customized peg-derived copolymers for tissue-engineering applications. Macromol. Biosci. 7 (1), 23–39.
Treloar, L.R.G., 1943. The elasticity of a network of long-chain molecules II. Trans. Faraday Soc. 39, 241–246.
Tsuji, H., 2002. Autocatalytic hydrolysis of amorphous-made polylactides: effects of L-lactide content, tacticity, and enantiomeric polymer blending. Polymer 43 (6), 1789–1796.
Tsuji, H., Ikada, Y., 2000. Properties and morphology of poly(L-lactide) 4. Effects of structural parameters on long-term hydrolysis of poly(L-lactide) in phosphate-buffered solution. Polym. Degrad. Stab. 67 (1), 179–189.
Tsuji, H., Mizuno, A., Ikada, Y., 2000. Properties and morphology of poly (L-lactide). iii. Effects of initial crystallinity on long-term in vitro hydrolysis of high molecular weight poly (L-lactide) film in phosphate-buffered solution. J. Appl. Polym. Sci. 77 (7), 1452–1464.
Vieira, A.C., Vieira, J.C., Ferra, J.M., Magalhães, F.D., Guedes, R.M., Marques, A.T., 2011. Mechanical study of PLA-PCL fibers during in vitro degradation. J. Mech. Behav. Biomed. Mater. 4 (3), 451–460.
Vieira, A.C., Guedes, R.M., Tita, V., 2014. Constitutive modeling of biodegradable polymers: hydrolytic degradation and time-dependent behavior. Int. J. Solids Struct. 51 (5), 1164–1174.
Wang, Y., Pan, J., Han, X., Sinka, C., Ding, L., 2008. A phenomenological model for the degradation of biodegradable polymers. Biomaterials 29 (23), 3393–3401.
Webb, A.R., Yang, J., Ameer, G.A., 2004. Biodegradable polyester elastomers in tissue engineering. Expert Opin. Biol. Therapy 4 (6), 801–812.